

# NUMERICAL INVESTIGATION OF THREE-DIMENSIONAL TRANSONIC FLOW WITH LARGE SEPARATION

M.A. Leschziner<sup>1</sup> and H. Loyau<sup>2</sup>

<sup>1</sup> Queen Mary and Westfield College, University of London, UK

<sup>2</sup> Aircelle, Harfleur, France

## Abstract

*Shock-induced separation is an extreme manifestation of strong shock/boundary-layer interaction. It is of substantial engineering interest in the context of transonic wings and turbomachine blades, because it alters significantly the operational characteristics of the component in question. Predicting this interaction is challenging, both from a numerical and turbulence-modelling point of view, especially when the flow is highly three-dimensional. This paper reports a computational study in which the performance of non-linear eddy-viscosity models is investigated when applied to a physically highly complex case of shock-induced separation in a duct flow over a swept bump inclined at 60° to the duct axis, followed by a shock-controlling second throat. The bump generates a skewed shock which interacts sensitively with the boundary layers on all four walls and causes extensive separation, strong transverse motion and highly complex topological flow features at the walls. The computations show that non-linear models yield a significantly more sensitive response of the boundary layers to the shock. This results in a better representation of the primary interaction processes, but also in excessively large transverse motion and hence insufficient rate of post-shock flow recovery. This is qualitatively consistent with observation in nominally 2D conditions, though the effect is much more pronounced in the present 3D case.*

## 1 Introduction

The interaction between a shock wave and a boundary layer is of considerable practical importance in the context of transonic-flow

conditions around civil-aircraft wings and in high-performance compressors. When the boundary layer is thin and the shock weak, the interaction is relatively benign, manifesting itself by a moderate thickening in the boundary layer and a minor influence on the essentially inviscid outer flow. However, a sufficiently strong shock will cause the boundary to decelerate strongly, possibly to the extent of separating, with consequent major alteration in the shock position and attendant changes to the pressure field (i.e. lift in aerofoils) and drag. In pronounced 3D conditions - as arising, for example, on the suction side of a swept wing - the shock also generates strong transverse motion (i.e. a major change in flow direction) due to streamwise deceleration.

The fundamentals of the above interaction are complex and ill-understood, and their practical manifestations are difficult to predict. With numerical and computer-resource issues set aside, the strength of the interaction is highly sensitive to the state of turbulence within the boundary layer and its response to the strong deceleration caused by the shock. In statistical terms, the turbulence field is highly anisotropic and responds quite differently to different types of straining - specifically, shear, normal and curvature strains. For example, strong shear causes turbulence levels to rise steeply, due to strong generation, while normal straining has a much weaker influence on the turbulence level. Curvature may cause turbulence to be damped or amplified, depending upon the state of normal-stress anisotropy in the flow and the sense of curvature relative to the strain field. From a numerical point of view, the main challenges

arise from the need to resolve acoustic effects, expressed by related influential characteristics of the conservation laws, and to secure numerical stability, convergence and economy in the solution of mixed hyperbolic-elliptic equations governing transonic flows. The latter is especially difficult in highly turbulent 3D flows modelled with advanced turbulence-transport closure

The practical importance of shock/boundary-layer interaction has provided strong impetus for a number of substantial computational investigations of a wide range of turbulence models in well-controlled, mostly 2D laboratory flows featuring strong interaction. Substantial efforts have been made, especially at NASA Ames in the early '90s (e.g. Menter [1], Marvin & Huang [2], Bardina *et al* [3]), to identify best modelling practices based on linear two-equation eddy-viscosity models for shock-affected flows. While these models are highly attractive on grounds of simplicity and economy and can be 'moulded' or tuned to return satisfactory predictions for a range of quite complex shock-affected flows, they are afflicted by a number of major fundamental weaknesses arising directly from the linear stress-strain relationship underpinning them. In particular, they are inherently unable to resolve anisotropy and to correctly represent the selective response of turbulence to different types of straining arising from the various linkages between any one stress and all strain components.

A class of models which that represent the above linkages are those based on the full second-moment transport equations, and such models have been the subject of much development and testing over the past few years. Recent investigations for shock-affected flows include those of Leschziner [4], Lien & Leschziner [5], Davidson [6], Vallet & Gerolymos [7] and Batten *et al* [8,9]. These have demonstrated that second-moment closure offers clear benefits over linear two-equation models, unless the latter are modified to include *ad-hoc* modifications and carefully tuned.

Second-moment models are complex, however, and their numerical properties pose severe challenges to numerical stability and economy.

The need to achieve a compromise between predictive accuracy and computational cost, especially in the context of industrial applications, has encouraged the development and use of an intermediate class of models which, whilst retaining the eddy-viscosity concept, adopt non-linear relationships between stresses and strain, and therefore include some of the linkages implied by the second-moment equations. It is this category of models that is the subject of the present paper.

Most past investigations of the predictive capabilities of alternative non-linear eddy-viscosity models have focused on incompressible flows (eg. Apsley *et al* [10]), while studies directed towards compressible flow are rare (Loyau *et al* [11], Barakos & Drikakis [12]). Moreover, all compressible flows investigated have been two-dimensional. Although no consensus has yet emerged on whether non-linear eddy-viscosity models, as a category, offers decisive practical advantages over simpler approaches, it is accepted that model forms *can* be constructed that resolve, realistically, normal-stress anisotropy, the weak response of turbulence to irrotational straining, relative to the strong response to shear straining, and the high sensitivity of turbulence to curvature strain. On the negative side of the balance, the precise nature of the non-linear stress-strain relationship and the values of the numerical coefficients attached to the various components of this relationship strongly influence the predictive performance of the models in different flow conditions. This is, arguably, a reflection of lack of fundamental rigour and an inevitable consequence of the major concessions made to simplicity, relative to complex interactions inherent in the exact second-moment equations.

The present paper reports the outcome of recent efforts to identify the benefits of using non-linear eddy-viscosity models for predicting shock/boundary-layer interaction in a strongly

three-dimensional flow related to the conditions around swept wings. The conditions considered - a ducted flow over a skewed bump - are much more complex, however, than those over a swept wing. It is, therefore, as searching a test case as almost any practical flow can be, at least from a physical point of view.

## 2 Modelling Considerations

Non-linear eddy-viscosity modelling for turbulent flows goes back to Lumley [13] and Pope [14], the latter proposing first an explicit, algebraic form of the Reynolds-stress closure from which transport terms are excluded. Several more recent variants have been derived along similar routes, evolving as successive simplifications to Reynolds-stress-transport models (Gatski & Speziale [15], Taulbee [16], Wallin & Johanson [17], Apsley & Leschziner [18]). In contrast, the starting point of other non-linear models (e.g. Shih *et al* [19], Craft *et al* [20]) has been the general non-linear, explicit expansion for the Reynolds-stress tensor in terms of the strain and vorticity tensors, in which the leading term corresponds to the conventional Boussinesq relations.

In principle, tensorial expansions of the above type can be developed to any order. However, these expansions are constrained, through the Cayley-Hamilton theorem, by the number of tensorially independent groups with coefficients that are functions of a finite number of tensorial invariants. Thus, a general and co-ordinate invariant cubic stress-strain relationship may be written in the following form:

$$\begin{aligned} \mathbf{a} = & -2f_\mu C_\mu \mathbf{s} + \beta_1 (\mathbf{s}^2 - s_2 \mathbf{I}) + \beta_2 (\mathbf{w}\mathbf{s} - \mathbf{s}\mathbf{w}) \\ & + \beta_3 \left( \mathbf{w}^2 - \frac{1}{3} w_2 \mathbf{I} \right) \\ & - \gamma_1 s_2 \mathbf{s} - \gamma_2 w_2 \mathbf{s} - \gamma_3 \left( \mathbf{w}^2 \mathbf{s} + \mathbf{s}\mathbf{w}^2 - w_2 \mathbf{s} - \frac{2}{3} \{\mathbf{w}\mathbf{s}\mathbf{w}\} \mathbf{I} \right) \\ & - \gamma_4 (\mathbf{w}\mathbf{s}^2 - \mathbf{s}^2 \mathbf{w}) \end{aligned} \quad (1)$$

where the following notation is used for second-rank tensors:

$$\mathbf{T} \equiv (T_{ij}), \quad \{\mathbf{T}\} \equiv \text{trace}(\mathbf{T}), \quad T_n \equiv \text{trace}(\mathbf{T}^n), \quad \mathbf{I} \equiv (\delta_{ij})$$

The *dimensional* mean-strain and mean-vorticity tensors are denoted in upper case by:

$$S_{ij} = \frac{1}{2} \left( \frac{\partial U_i}{\partial x_j} + \frac{\partial U_j}{\partial x_i} \right), \quad W_{ij} = \frac{1}{2} \left( \frac{\partial U_i}{\partial x_j} - \frac{\partial U_j}{\partial x_i} \right),$$

whilst *dimensionless* quantities - anisotropy  $\mathbf{a}$ , mean strain  $\mathbf{s}$  and mean vorticity  $\mathbf{w}$  - are written in lower case and defined by:

$$a_{ij} = \frac{\overline{u_i u_j}}{k} - \frac{2}{3} \delta_{ij}, \quad s_{ij} = \frac{k}{\varepsilon} S_{ij}, \quad w_{ij} = \frac{k}{\varepsilon} W_{ij}$$

For compressible flows, it is assumed that  $S_{ij}$  may be replaced by:

$$S_{ij}^* = S_{ij} - \frac{1}{3} S_{kk} \delta_{ij} \quad (2)$$

The models used in computations to follow all use forms of  $k$  and  $\varepsilon$  equations, which may be written in the general form as:

$$\begin{aligned} \frac{\partial}{\partial t} (\rho k) + \frac{\partial}{\partial x_j} (\rho U_j k) \\ = \frac{\partial}{\partial x_j} \left[ \left( \mu + \frac{\mu_t}{\sigma_k} \right) \frac{\partial k}{\partial x_j} \right] + \rho (P - \varepsilon - D) \end{aligned} \quad (3)$$

$$\begin{aligned} \frac{\partial}{\partial t} (\rho \varepsilon) + \frac{\partial}{\partial x_j} (\rho U_j \varepsilon) \\ = \frac{\partial}{\partial x_j} \left[ \left( \mu + \frac{\mu_t}{\sigma_\varepsilon} \right) \frac{\partial \varepsilon}{\partial x_j} \right] \\ + \rho (C_{\varepsilon 1} f_1 P - C_{\varepsilon 2} f_2 \varepsilon) \frac{\varepsilon}{k} \\ + \rho (S_\ell + S_\varepsilon) \end{aligned} \quad (4)$$

where the coefficients, the functions  $f$  and the terms  $D$ ,  $S_\ell$  (the "Yap" correction) and  $S_\varepsilon$  (procuring the correct limiting behaviour of  $\varepsilon$  in

the viscous sublayer), if not zero, depend on the particular model variant used (for details see Loyau *et al* [11], Apsley and Leschziner [21]).

It may be readily demonstrated (see Apsley *et al* [18]) that the quadratic terms in (1) allow anisotropy to be represented, while the cubic terms provide a means for sensitising the stresses to the stabilising as well as destabilising effects of curvature strain and swirl. However, the level of these interactions depends greatly on the coefficients which are typically derived by calibration against experimental or DNS data for key flows. Calibration is not merely confined to the coefficients of the stress-strain relationship, but extends to the transport equation governing the length scale or a related quantity. All models considered herein use the rate of dissipation,  $\varepsilon$ , as the length-scale variable, but the precise form of the equation used in different models vary.

One important and well-known defect of standard forms of linear eddy-viscosity models is that they predict a strong rise of turbulence energy and viscosity in response to normal straining. This can be traced directly to the replacement of the normal stresses by the normal strains through the Boussinesq relations. As a result of this substitution, the rate of turbulence energy production rises irrespective of the sign of the normal strains, i.e. all normal-strain components reinforce the production rate, which is contrary to reality. Non-linear eddy-viscosity models share this weakness with their linear counterparts, because the leading term of the former is simply the latter. To remove this weakness, the coefficient  $C_\mu$  multiplying the linear strain term must be made to depend on strain and vorticity invariants so as to yield a progressive decline in its value when the flow is subjected to irrotational and also strong shear straining, the latter beyond the value at which local turbulence equilibrium is maintained.

All non-linear models have been formulated and calibrated by reference to incompressible flows, and the question of their applicability to compressible conditions arises

especially in relation to shock-affected flows. One modification, at mean-flow level, has already been included through substitution (2). The effects of compressibility on turbulence and their consequence on the closure approximation and the calibration of the model coefficient is a more difficult issue.

At Mach numbers below about 5 - a condition satisfied for the applications to follow - the Morkovin Hypothesis (Morkovin [22]) implies that effects of density fluctuations are small. Additional effects arise from dilational dissipation and pressure-strain contributions which emerge from the exact derivation of the dissipation and stress-transport equations (see Coakley *et al* [23]). Several compressibility corrections to incompressible closure forms, mainly at eddy-viscosity level, have thus been proposed for these contributions. However, Huang *et al* [24] have shown convincingly, on the basis of an analysis of DNS data for compressible boundary layers, that the wall strongly suppresses the effects of compressibility on turbulence and that all proposed compressibility corrections are inapplicable to near-wall layers. For this reason, no compressibility corrections, beyond those associated with mean-flow dilatation, have been used in computations to follow.

### 3 Numerical Methodology

Computational results presented below have been obtained with a structured-grid, finite-volume scheme developed by Batten *et al* [25]. This is an implicit scheme based a Harten/Lax/van-Leer average-state approximation to the exact Riemann problem. The mean-flow conservation laws are solved in a fully-coupled fashion, while the turbulence equations are solved as a separate sub-set, but are coupled to the mean-flow set by way of source terms and viscous-transport terms. The scheme has been used to compute a wide range of compressible 2D and 3D flows with second-moment closure (Batten *et al* [8, 9]) and non-

linear eddy-viscosity models (Loyau et al [11]).

## 4. Validation

### 4.1 Geometry and Computational Details

The test case under consideration is a transonic flow in a rectangular duct with a bump on the lower wall, inclined at  $60^\circ$  relative to the duct axis, as shown in Fig. 1. The bump creates a sonic throat which accelerates the flow from Mach 0.8 to a maximum of about 1.75. The shock position is controlled by a second throat which re-accelerates the flow to supersonic speed. Experiments for this case were performed by Pot *et al* [26] at ONERA, with extensive data being obtained for pressure, surface-flow topology, velocity and second moments, the last two with two-colour LDA techniques.

Computations were initially performed on a truncated geometry, with the computational exit placed between the bump and the second throat. This is a practice widely adopted in several earlier investigations of the nominally 2D transonic bump flows ("A", "B" and "C") of Delery [27] in which the bumps are at  $90^\circ$  to the flow. In these cases, the experimentally recorded pressure was prescribed at the exit boundary condition, and this has been shown by Leschziner *et al* [28], on the basis of comparative computations for the full and truncated geometries, to be entirely adequate. However, in the present 3D geometry, it quickly transpired that the practice of prescribing a uniform exit pressure was untenable, because the skewed bump generated large transverse motions accompanied by large cross-flow pressure variations. Hence, the only approach held to offer the promise of a sufficient degree of correspondence between experiment and calculation is one of computing the full geometry with the second throat included.

Results reported below were obtained with a grid of 122x60x55 nodes. To check grid-dependence, some computations were repeated on a 202x90x85 grid (1.6M nodes). This

resolution is better than that known to give essentially grid-independent results in earlier 2D-bump-flow computations. Differences between corresponding solutions were found to be minor, but not wholly negligible. Although it would have been preferable to use the finer grid for all computations, this was not possible because of the very high CPU demands, despite the implicit nature of the numerical scheme. Particular difficulties arose from the very high sensitivity of the flow field to even slight changes in the height of the second throat (which is not known accurately), from the fact that the Mach number between the two throats, following the shock, was very close to unity, and from the strong transverse motion.

### 4.2 Results

Computational solutions were obtained for 6 models:

- Lien & Leschziner's linear k- $\epsilon$  model [29] ("LL");
- Menter's linear SST model [1] ("SST");
- Craft *et al*'s cubic model [20] ("CLS");
- Two variants of Lien *et al*'s cubic model [30] ("LCL" and "LCL\*");
- Apley and Leschziner's cubic model [31] ("AL").

The last model, SST, has been included because it is regarded, in the aeronautical community, as the best linear model two-equation model for compressible external aerodynamic flows. The first model, LL, is among the best 'standard' low-Re  $k$ - $\epsilon$  model, i.e. those not containing *ad-hoc* corrections for specific flow characteristics.

Space constraints prevent more than a few sample results from being included here. In most figures, the focus is on comparisons between the cubic CLS model and the linear LL model, the former often found to return better predictive performance than other non-linear models in incompressible flows.

Fig. 2 gives colour maps of the Mach-number fields predicted by all 6 models across the spanwise midplane of the channel. All

models are seen to return a highly pronounced lambda-shock structure in the primary interaction region, and this feature varies little across the model range. Important differences in the flow fields are indicated, however, by the extent of the red regions immediately downstream of the normal leg of lambda shock. These regions indicate a relatively high Mach number and signify slower post-shock recovery. As will be seen below, there are also corresponding, material differences in the bump-pressure variations downstream of the shock which are associated with the post-shock Mach number. In general, the non-linear models predict a significantly lower post-shock recovery than the standard linear model, while the SST model appears to return a behaviour that is qualitatively similar to that predicted by the non-linear models.

Fig. 3 shows iso-Mach contours in the primary interaction region predicted by one linear and the cubic CLS model in comparison with experimental fields at two spanwise planes. The left-hand-side plots relate to the duct-centre plane and demonstrate that the lambda shock structure is well resolved by both models with the computed fields resembling closely to each other. However, this comparison hides some very substantial differences in model performance, which only come to light when attention is turned to a range of other results. Thus, the right-hand-side plots in Fig. 3, which pertain to a near-side-wall plane, bring to light some large differences in the predicted flow fields, and these reflect corresponding differences in the post-shock region, especially in respect of the level of the transverse motion induced by the skewness of the shock relative to the flow direction.

Fig. 4 shows bump-wall pressure distributions at 2 out of 6 spanwise planes documented in Loyau and Leschziner [32]. These distributions reveal that the non-linear CLS model as well as the SST model represent significantly better than the linear  $k-\varepsilon$  model the intricate details of the interaction process. However, these same models fail to return the

correct recovery in the post-shock region, and this general conclusion is reinforced by further comparisons of pressure at the upper and side walls which are not included here. The AL model predicts solutions which lie in-between those returned by the linear  $k-\varepsilon$  model and the cubic CLS model.

Predictive weaknesses in the post-separation region is a recurring theme, in 2D as well as 3D flows, but the problem is here complicated and aggravated by the fact that the non-linear models tend to predict very large transverse motions in the post-shock recovery region. This is well brought out in Fig. 5 which compares skin-friction lines along the upper and lower walls and the front side wall. On the bump wall, both the linear and the cubic models return a qualitatively correct flow topology, characterised by a single dominant focus. However, on the upper and especially on the side walls, the models predict quite different behaviour. Thus, the cubic CLS model returns (like the other models examined) large separated regions close to the upper wall and in one upper-duct corner. It is this motion, again reflecting higher sensitivity to the shock, that is associated with the low rate of pressure recovery between the two throats.

### Concluding Remarks

The sensitive interaction between a strong oblique shock and the turbulent flow in a duct gives rise to extremely complicated flow and surface-topology features. In fact, the flow is much more complex than the practical application it is meant to represent, namely the conditions on the suction side of a transonic swept wing. The flow is multiply-separated, involves very large curvature, large spanwise motion and large streamwise vorticity. These conditions are extremely challenging, both physically and computationally, and the flow is therefore a searching test case for any turbulence model.

The main conclusion emerging from the study is that non-linear eddy-viscosity models

return a significantly better resolution than standard linear ( $k$ - $\epsilon$ -based) forms of the complex interaction processes in the immediate vicinity of the shock, but fail to represent correctly the recovery process. This weakness is associated with the prediction of excessive transverse motion and reverse flow close to walls, implying an insufficient level of mixing in this region. Similar defects are also observed in linear models that include modifications designed to suppress the eddy viscosity so as to return the correct separation behaviour. Apparently, then, the calibration of models by reference to their ability to return the separation behaviour correctly is damaging to their predictive capabilities in the recovery region.

#### **Acknowledgement:**

The authors are grateful to BAE Systems and DERA for their financial support.

#### **References**

- [1] Menter F R. *J. AIAA*, Vol. 32, pp. 1598-1605, 1994.
- [2] Marvin J G and Huang P G. Turbulence modelling - progress and future outlook, *Proc. 15th Conf. on Numerical Methods in Fluid Dynamics*, Monterey, California, 1996.
- [3] Bardina J E, Huang P G and Coakley T J. Turbulence modelling validation, testing and development, *NASA TM-110446*, 1997.
- [4] Leschziner M A. ONERA bumps A and C, *Notes on Numerical Fluid Mechanics* (W Haase et al, Eds) pp. 187-265, 1993.
- [5] Lien F-S and Leschziner M A. *J. of Fluids Engineering*, Vol. 115, pp. 717-725, 1993.
- [6] Davidson L. *Computers & Fluids*, Vol. 24, pp. 253-268, 1995.
- [7] Vallet I and Gerolymos G A. *Computational Fluid Dynamics '96*, Wiley, pp. 167-173, 1996.
- [8] Batten P, Craft T J, Leschziner M A and Loyau H. *J. AIAA*, Vol. 37, pp. 785-797, 1999.
- [9] Batten P, Leschziner M A, Craft T J. Reynolds-stress modelling of afterbody flows, *Proc. 1st Symp. of Turbulence and Shear Flow Phenomena* (S. Banerjee and J. Eaton Eds.), pp. 215-220, 1999.
- [10] Apsley D D, Chen W-L, Leschziner M A, and Lien F-S. *IAHR J. of Hydraulic Research*, Vol. 35, pp. 723-748, 1998.
- [11] Loyau H, Batten P and Leschziner M A. *Flow, Turbulence and Combustion*, Vol. 60, pp. 257-282, 1998.
- [12] Barakos G and Drikakis D. Investigation of non-linear eddy-viscosity models in shock/boundary-layer interaction, to appear in *J. AIAA*, 2000.
- [13] Lumley J L. *J. Fluid Mech.*, Vol. 41, pp. 413-434, 1970.
- [14] Pope S B. *J. Fluid Mech.*, Vol. 72, pp. 331-340, 1975.
- [15] Gatski T B and Speziale C G. *J. Fluid Mech.*, Vol. 254, pp. 59-78, 1993.
- [16] Taulbee S. *Phys. Fluids A*, Vol. 4, pp. 2555-2561, 1992.
- [17] Wallin S and Johansson A V. A new explicit algebraic Reynolds-stress turbulence model for 3D flows, *Proc. 11th Symp. on Turbulent Shear Flows* (F. Durst et al, Eds.), Grenoble, France, pp. 13.13-13.17, 1997.
- [18] Apsley D D and Leschziner M A. *Int. J. Heat Fluid Flow*, Vol. 19, pp. 209-222, 1998.
- [19] Shih T-H, Zhu J and Lumley J L. A realizable Reynolds stress algebraic equation model, *NASA TM-105993*, 1993.
- [20] Craft T J, Launder B E and Suga K. *Int. J. Heat Fluid Flow*, Vol. 17, pp. 108-115, 1996.
- [21] Apsley D D and Leschziner M A. Advanced turbulence modelling of separated flow in a diffuser, *Flow, Turbulence and Combustion* (in press), 2000.
- [22] Morkovin, M V. Effects of compressibility on turbulent flows, *Mecanique de la Turbulence* (A. Favre Ed.), Gordon and Breach publ., NY, pp. 367-380, 1962.
- [23] Coakley T J, Horstman C C, Marvin J G, Viegas J R, Bardina J E, Huang P G and Kussoy M I. Turbulence compressibility corrections, *NASA TM-108827*, 1994.
- [24] Huang P G, Coleman G N and Bradshaw P. *J. Fluid Mech.*, Vol. 305, pp. 185-218, 1995.
- [25] Batten P, Leschziner M A and Goldberg U C. *J. Comp. Phys.*, Vol. 137, pp. 38-78, 1997.
- [26] Pot T, Delery J and Quelin C. Interaction choc-couche limite dans un canal tridimensionnel - nouvelles experiences en vue de la validation du code CANARI, *ONERA TR-92/7078 AY*, 1991.
- [27] Delery J. Investigation of strong turbulent boundary-layer interaction in 2D flows with emphasis on turbulence phenomena, *Paper AIAA 81-1245*, 1981.
- [28] Leschziner M A, Loyau H and Apsley D D. Prediction of shock/boundary-layer interaction with non-linear eddy-viscosity models, *Proc. ECCOMAS 2000*, Barcelona (to appear), 2000.
- [29] Lien F-S and Leschziner M A. *Int. J. CFD*, Vol. 12, pp. 1-12, 1999.

- [30] Lien F-S, Chen, W-L and Leschziner, M.A. *Engineering Turbulence Modelling and Experiments 3*, (W. Rodi and G. Bergeles, Eds.). Elsevier, pp. 91-100, 1996.
- [31] Apsley, D.D. and Leschziner, M.A. *Int J Heat and Fluid Flow*, Vol. 19, pp. 209-222, 1998.
- [32] Loyau H and Leschziner M A. Computational modelling of 3D separated transonic flows pertinent to aerodynamics with advanced turbulence-transport models, *Final Project Report submitted to DERA and BAE Systems (Restricted)*, 1999.

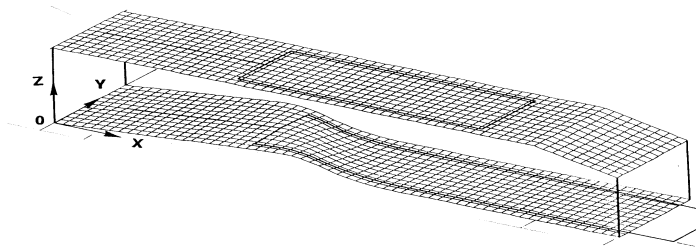


Fig. 1: Swept-bump geometry with second downstream throat

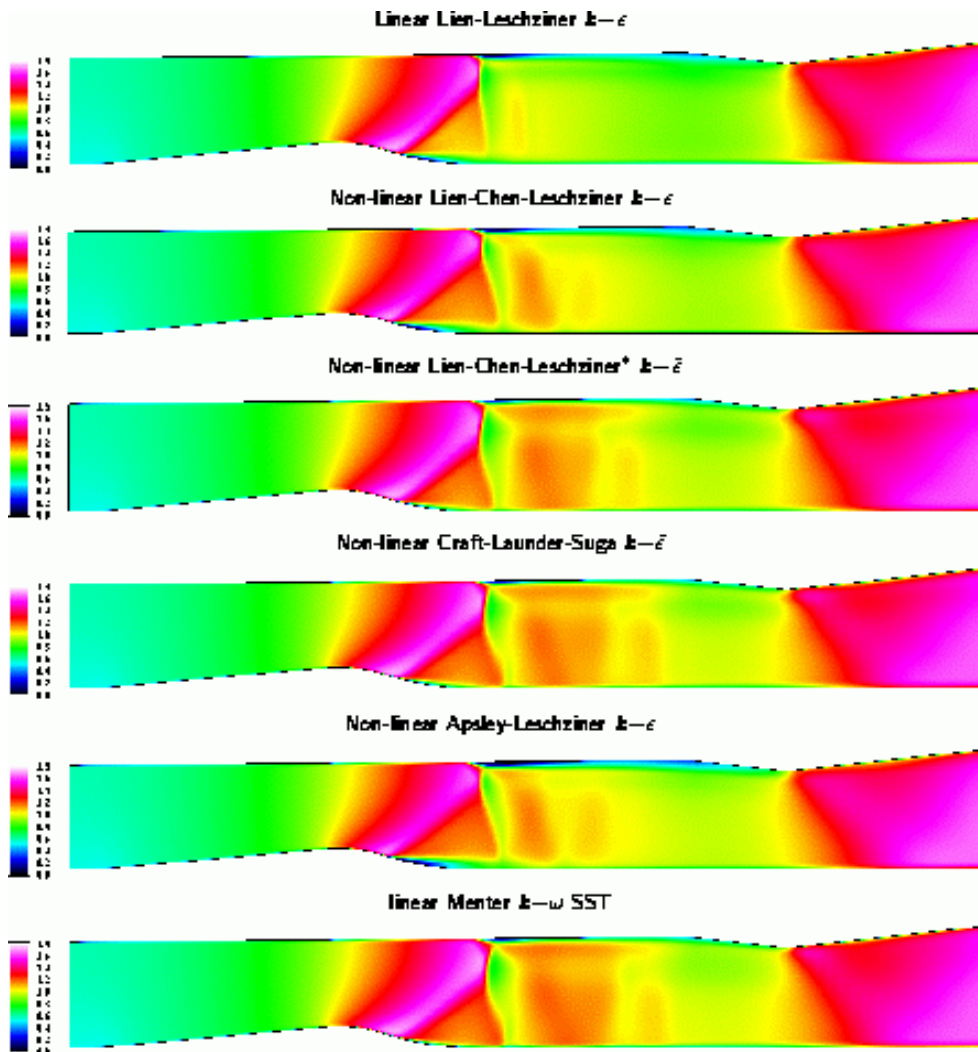


Fig. 2: Mach fields across spanwise mid-plane of channel



## NUMERICAL INVESTIGATION OF THREE-DIMENSIONAL TRANSONIC FLOW WITH LARGE SEPARATION

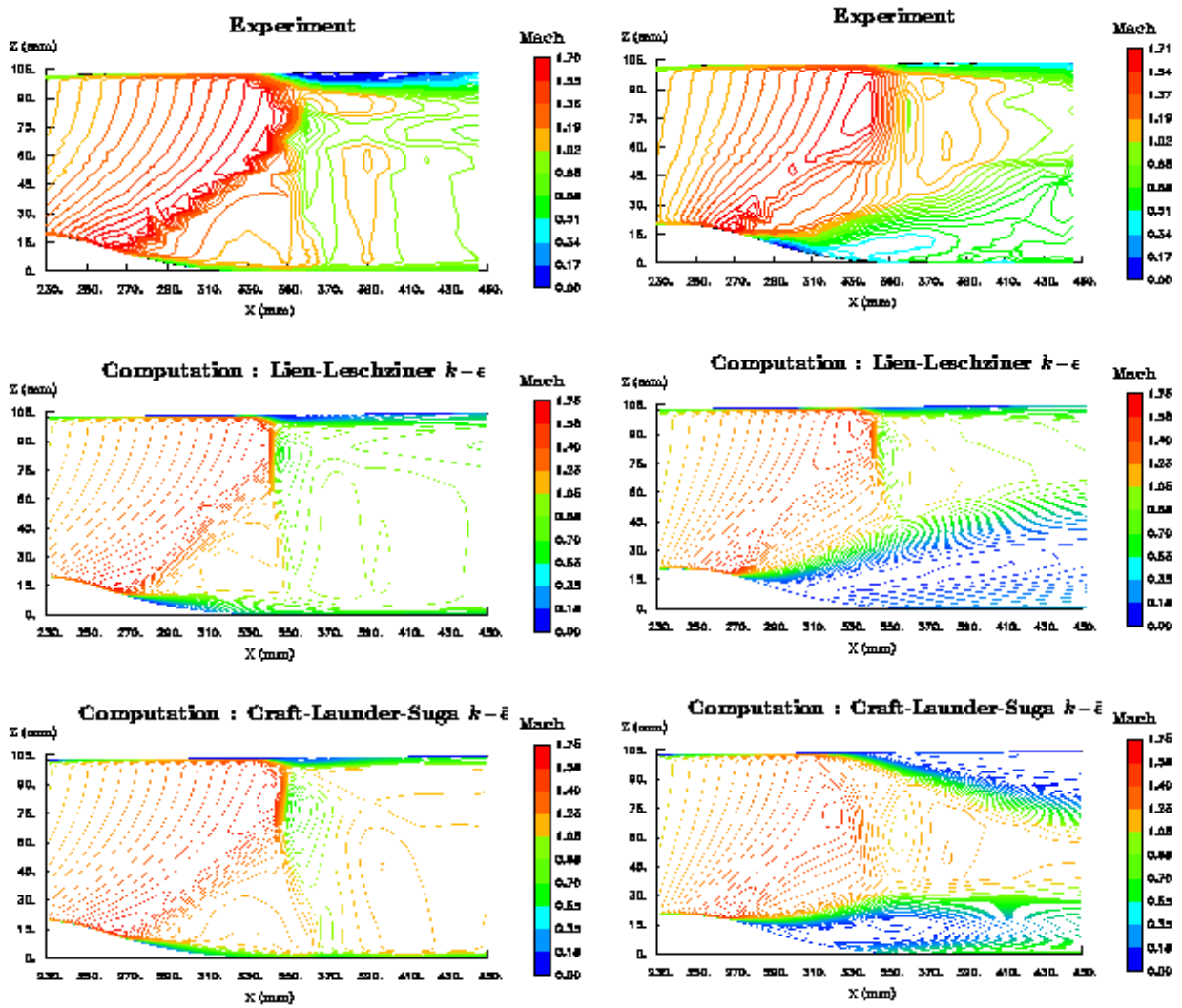


Fig. 3: Mach-contours across spanwise mid-plane (lhs) and plane close to front side wall (rhs)

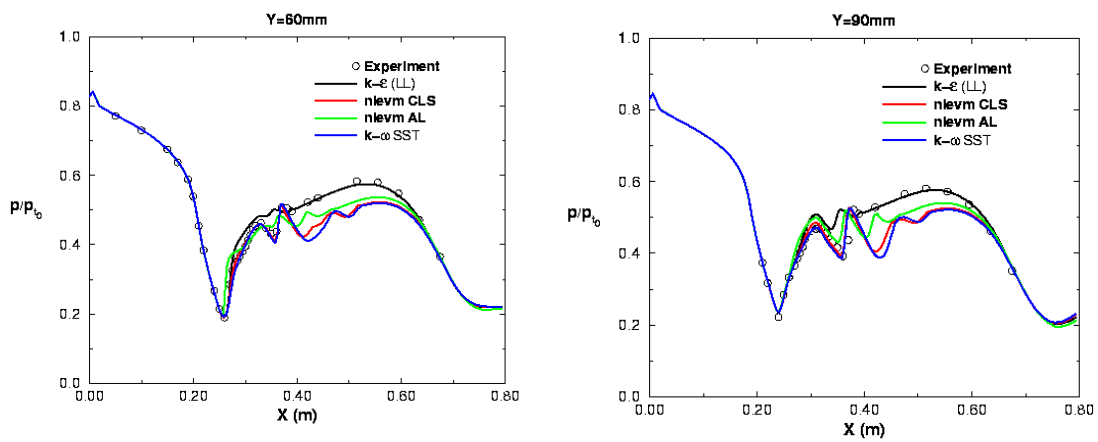


Fig. 4: Pressure distributions on bump wall at two spanwise planes

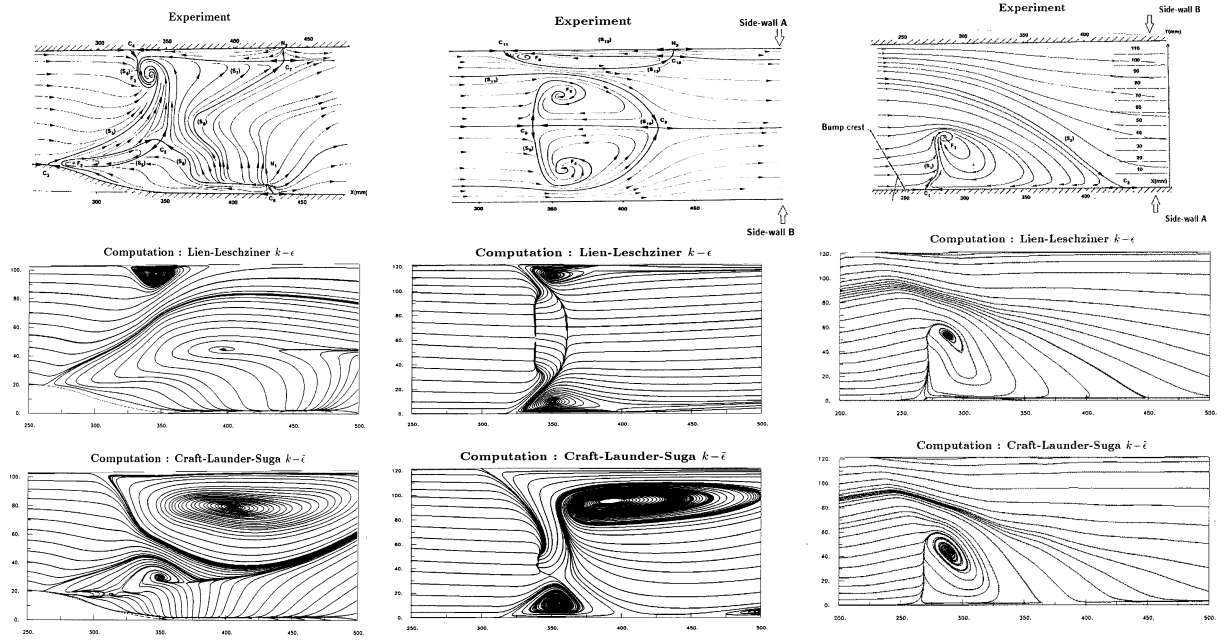


Fig. 5: Skin-friction lines (flow topology) on front side wall (lhs), upper wall (middle) and bump wall (rhs)